

Research Article

# Comparing Different Fiber Guided Light Delivery Strategies in an Endocavity Photoacoustic Imaging System: A Monte-Carlo Simulation Study

Yan Yan<sup>1#</sup>, Sirisha Kondle<sup>2#</sup>, and Mohammad Mehrmohammadi<sup>1,2,3\*\*</sup>

<sup>1</sup>Department of Biomedical Engineering, Wayne State University, USA

<sup>2</sup>Department of Electrical Engineering, Wayne State University, USA

<sup>3</sup>Barbara Ann Karmanos Cancer Institute, USA

**\*Corresponding author:** Mohammad Mehrmohammadi, Department of Biomedical Engineering, Wayne State University, Detroit, Michigan, USA, Tel: +313-577-8883; E-mail: [mehr@wayne.edu](mailto:mehr@wayne.edu)

**Received:** May 18, 2019; **Accepted:** July 02, 2019; **Published:** July 09, 2019

**Copyright:** ©2019 Mehrmohammadi M, et al. This is an open access article distributed under the Creative Commons Attribution License, which permits unrestricted use, distribution, and reproduction in any medium, provided the original work is properly cited.

**Citation:** Yan Y, Kondle S, Mehrmohammadi M (2019) Comparing Different Fiber Guided Light Delivery Strategies in an Endocavity Photoacoustic Imaging System: A Monte-Carlo Simulation Study. J Biomed Res Prac 2(1): 100015.

## Abstract

Photoacoustic (PA) imaging is a novel ultrasound-based imaging modality which has shown tremendous diagnostic potential by providing complementary functional and molecular information. PA imaging utilizes short laser pulses to excite the tissue and probes its optical properties. Fiber guided light delivery is the most common approach for clinical PA imaging devices due to its high flexibility and ease of maintenance. It is always a challenge during the design and development of a new PA device to maximize the PA imaging penetration depth with limited fibers. In this paper, we evaluated two key parameters which affected the PA imaging penetration depth, the initial light intensity, and illumination directionality, by using a 3D Monte-Carlo based light simulation. We performed several sets of virtual tissue-mimicking phantom simulations to quantify the effects. We demonstrated the fiber size (initial light intensity) had insignificant effects for PA penetration depth under the condition of the different core-size fibers covered similar illumination diameter. We also indicated the initial light beam direction (illumination directionality) has significant impacts for the PA imaging depth. We compared several illumination patterns revolving around a clinical endocavity ultrasound (US) probe, the focused strategy which focused the light energy towards the US imaging plane and non-focused strategy. Based on our simulation results, we can indicate that the focused light delivery strategy has the ability to image twice the depth than the non-focused. We concluded during the design and development of any new integrated US and PA imaging system, the capability of the design to focus the delivered light more towards to the center of US imaging plane can potentially increase the PA imaging depth within the fiber and fluence limitations.

**Keywords:** photoacoustic, illumination design, fiber optic

## Introduction

Photoacoustic (PA) imaging is an application of optoacoustic effect which was first explored by Alexander Graham Bell in 1880 [1]. Physics and chemistry researchers initially used and studied photoacoustic techniques in

non-biological fields [2]. Since Theodore Bowen introduced PA imaging technique as a biomedical imaging modality in 1981 [3], this technology has been developing quite rapidly by several early adopters of photoacoustic imaging [4,5]. Fundamentally, the photoacoustic technique measures the conversion of electromagnetic energy into Acoustic Pressure Waves (APW). In biomedical PA imaging, the tissue is irradiated with a nanosecond pulsed laser, resulting in the generation of an ultrasound wave due to optical absorption and rapid thermal expansion of tissue [2]. The amplitude of APW which is received by an ultrasound probe and usually defined as PA signal amplitude which is a positive correlation with the amount of electromagnetic energy delivered at its location. Therefore, the PA signal amplitude is proportional to the fluence which is distributed inside the target tissue. The challenge for designing an integrated ultrasound (US) and PA imaging system is the optimization of the light delivery system with limited fibers and fluence [6]. There are two key factors in the design, initial light intensity, and illumination directionality. Initial light intensity is the initial illumination area determined by the fiber core-size. The illumination directionality is the beam direction exiting the fiber. Researchers had created a variance of simulation methods based on Monte-Carlo algorithm, which is a flexible method to simulate randomized light propagation within the tissue [7-11]. The approach of Monte-Carlo method simulates the photons randomly traveling inside the tissue depending on the statistical sampling probability distributions. These probability distributions are estimated for each step size and angular deflection per scattering. After transmitting many photons, the net distribution of energy yields an accurate approximation [12-14]. By using Monte-Carlo light simulation method, it can accurately simulate the light fluence delivered inside tissue mimicking phantoms and real biological tissues based on the defined light delivery strategy.

In this paper, we used a Monte-Carlo based light simulation program to perform several simulation studies to indicate the initial light intensity and illumination directionality effects in fiber-guided light delivery around a clinical endocavity US probe. We studied the fiber core-size (initial light intensity) and beam direction (illumination directionality) effects for PA imaging depth. We found the optimized light delivery strategy for an endocavity US probe (C9-5, ATL) which can potentially increase the PA imaging depth within the clinical and laser safety limitations.

## **Materials and Methods**

### **Effect of initial illumination intensity on PA penetration depth**

Initial light intensity is a key factor to indicate the penetration of light in the scattering medium [15]. In a fiber guided light delivery system, the initial light intensity is determined by the fiber core-size. To evaluate the effect of fiber diameter, two scenarios were demonstrated, (1) large core-size fiber with a diameter of 1 mm and (2) five small core-size, 200  $\mu\text{m}$  fiber covering the same diameter of illumination, Figure 1a. The simulation block diagram is shown in Figures 1b and 1c. The simulations are performed in a virtual human tissue-mimicking phantom. The phantom is a volumetric cube of side 50 mm. There are four layers within the simulated phantom, the first layer is the escape layer for photons, followed by 5 mm space filled with water and the remaining amount is filled with human tissue. A blood vessel was located within the virtual phantom, at a depth of 25 mm from the surface of the human tissue. The radius of the blood vessel is 2.5 mm. The simulation beam wavelength was selected at 680 nm within the PA imaging range for imaging deep biological tissues [16,17]. The optical properties of the simulated phantom were adopted from [7,18-24]. The simulated energy at the surface of the phantom is about 20 mJ/cm<sup>2</sup>. The simulated energy lies within the laser safety requirements [6] and close to the clinical application.

### **Effect of illumination directionality on PA penetration depth**

Illumination directionality is also a key parameter which describes the path of light traveled inside the tissue [15]. In clinical PA imaging, the highly collimated laser beams entering the highly scattering human tissue are immediately diffused, lose their directionality [23,25], and affects the photon distribution possibility which leads to

different PA imaging penetration depth [26]. The distribution changes in photon path by different illumination directionality (beam direction), was evaluated by creating several illumination patterns around a clinical transvaginal US probe (TVUS), ATL C9-5.

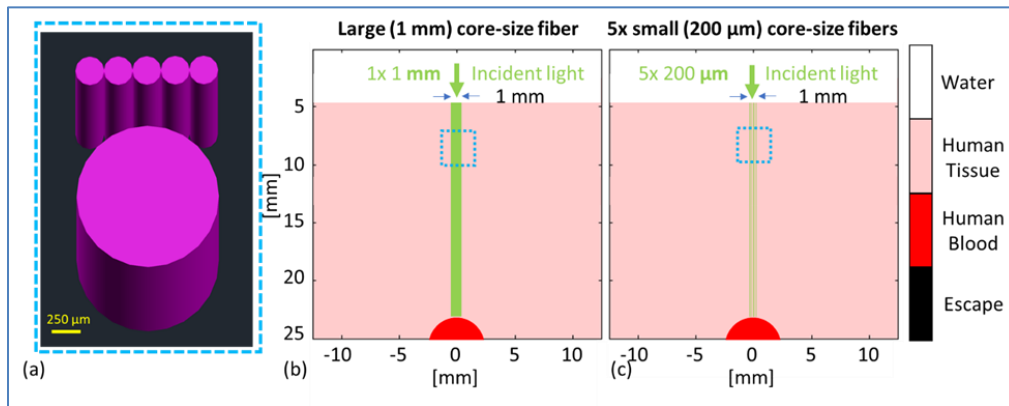


**Figure 1:** Diagrammatic simulation scenarios indicating the effect of different fiber core-size on initial illumination intensity to PA imaging penetration depth.

The TVUS probe has a radius of  $\sim 1.5$  cm and each side of the aperture consisted of an arc length  $\sim 20$  mm which can be used for aligning 18 large core-size fibers. Several scenarios of simulation studies (focused and non-focused) were performed to evaluate the effect of illumination direction to the PA imaging penetration depth. In the non-focused alignment strategy (Figure 2a), the fibers were equally placed around the arc of the probe and the laser beams from the fibers were directed along the same direction of the transmitted US waves. Similar to the non-focused alignment strategy, focused illumination strategy also consisted of equally aligned fibers at each side of the probe (Figure 2b), but each fiber had an individual bending angle to form a focused illumination line at 25 mm away from the transducer surface towards the center of the probe. Figures 2c and 2d show the transverse view at the center plane of the simulations. In both simulations, the fiber core-size is 1 mm and the distance between the two fiber is 0.2 mm. The virtual tissue mimicking phantom used in the simulations have the same optical parameters as shown before.

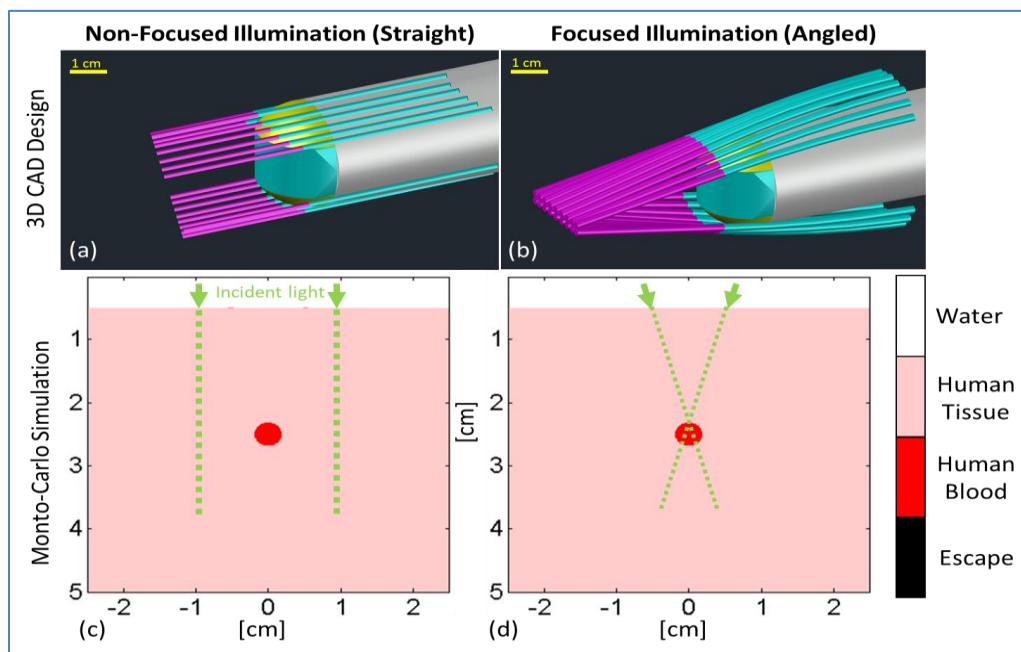


**Figure 2:** Diagrammatic simulation scenarios indicating the effect of different beam direction on illumination directionality to PA imaging penetration depth.

## Results and Discussion

The simulated fluence results in the virtual phantom for indicating the effects of initial illumination intensity are shown in Figures 3a-3d. The color map of the images presents the fluence intensity. We also calculated the simulated fluence to compare the different initial illumination and plotted in Figure 3e. From those results, we can indicate there is an insignificant difference between large core size and small core size scenarios with the illumination area and averaged fluence intensity.

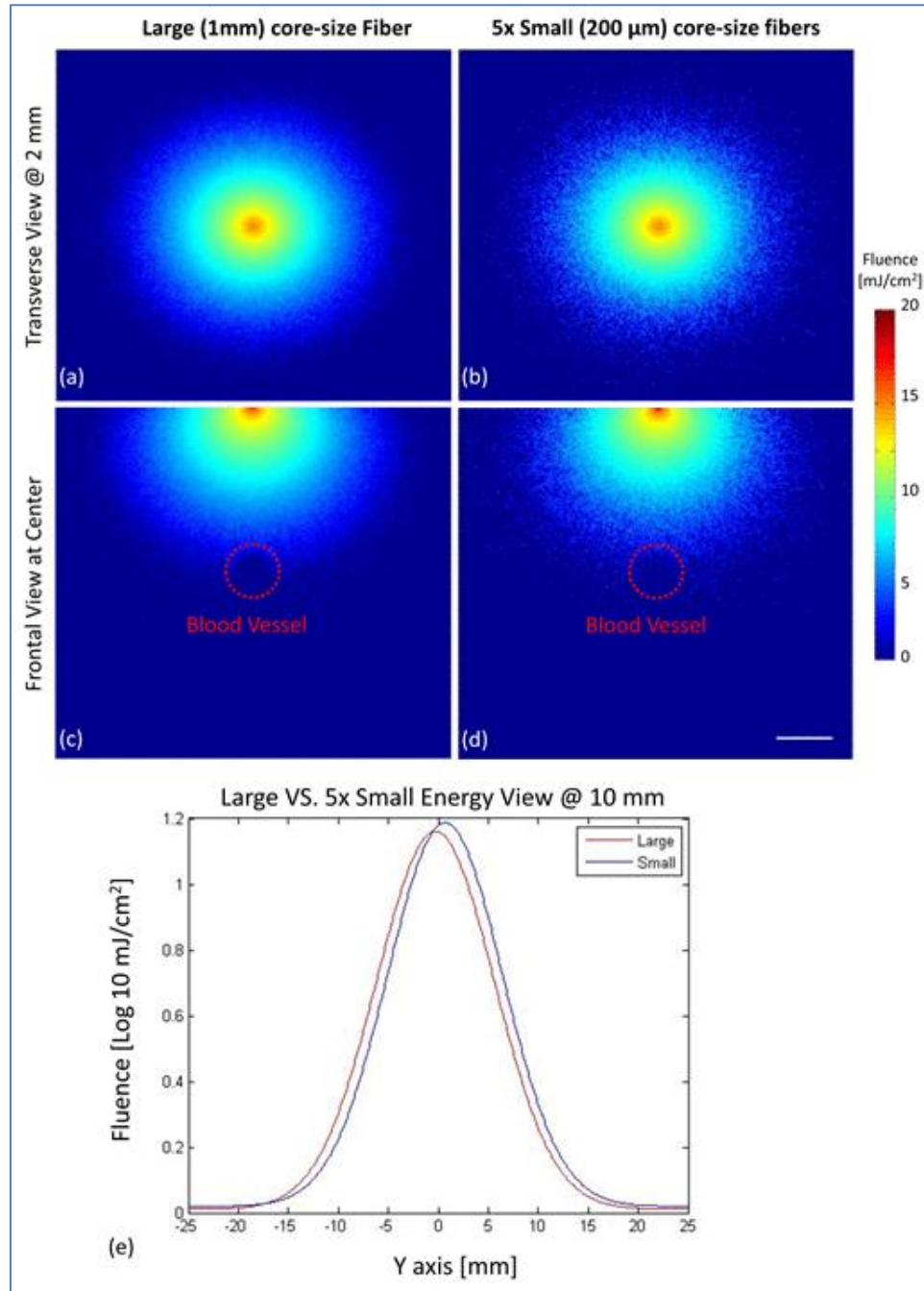


**Figure 3:** Results of Monte-Carlo simulation indicating the effect of different fiber core-size on PA imaging penetration depth. Left panel indicates the fluence results from large core-size fiber (1 mm). Right panel indicates the fluence results from 5 small core-size (200  $\mu\text{m}$ ) fibers, (a, b) Transverse view at 2 mm depth. (c, d) Frontal view from the center. (e) Gaussian fitted energy distribution curves at a depth of 10 mm at the center line for the two illumination strategies. The scale bar indicates 10 mm.

The Full Width Half Maximum (FWHM) of these two scenarios has a different less than 5%. In Figure 4, shows the simulation results for indicating the illumination directionality effects for PA imaging penetration depth. In Figures 4a-4f shows the colored fluence distribution in the simulation results. From Figures 4c and 4d we can easily identify there is more fluence delivered in the focused light illumination compare to the non-focused at 25 mm deep inside the phantom. To quantitatively compare the energy difference, we calculated the fitted Gaussian curve represent the light intensity at 10 mm deep inside the tissue (Figure 4g). From the Gaussian fitted fluence curve, there is a significant difference in energy distribution between those two scenarios. The intensity of focused illumination delivered five times more energy than the non-focused illumination. Therefore, we can conclude that the directionality of the laser beam has effects for the PA imaging penetration depth. By targeting the initial beam direct more towards the desired imaging object gives higher PA imaging penetration depth.

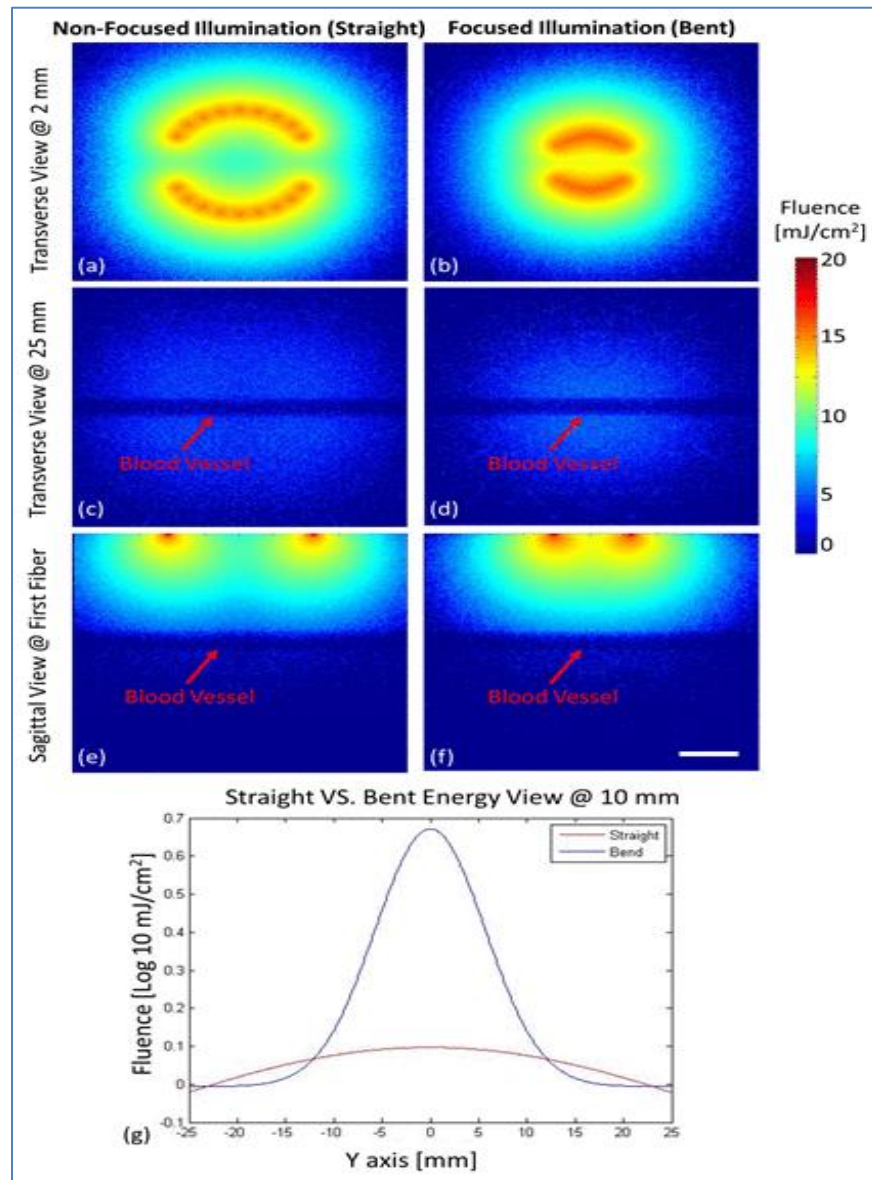


**Figure 4:** Results of Monte-Carlo simulation indicating the effect of different initial beam direction on PA imaging penetration depth. Left panel indicates the fluence results from non-focused illumination strategy. Right panel indicates the fluence results from focused illumination strategy. (a, b) Transverse view at 2 mm depth. (c, d) Transverse view at 25 mm depth. (e, f) Sagittal view at the centermost (first) fiber. (g) Gaussian fitted energy distribution curves at a depth of 10 mm at center line for the two illumination strategies. The scale bar indicates 10 mm.

## Conclusion

A series of Monto-Carlo simulation studies were performed to indicate the initial illumination intensity and directionality effects for PA imaging penetration depth. The results stipulated that the fiber core-size has insignificant effects for the penetration depth of PA under the condition where the different core-size fiber covering the same illumination diameter. The initial beam direction has a significant impact on the penetration depth of PA imaging. The design and development of any integrated US and PA imaging system revolve around the ability of the designed system to focus their fiber-guided illumination pattern towards the acoustic imaging plane of their transducer, which may lead to a higher PA imaging penetration depth.

## Conflict of Interest

The authors declare that there exists no conflict of interest.

## References

1. Bell AG (1881) The production of sound by radiant energy. *Science* 28: 242-253.
2. Rosencwaig A, Gersho A (1976) Theory of the photoacoustic effect with solids. *J App Physics* 47: 64-69.
3. Bowen T (1981) Radiation-induced thermoacoustic soft tissue imaging. *Ultrasonics Symposium*; Chicago, USA.
4. Xu MH, Wang LHV (2006) Photoacoustic imaging in biomedicine. *Rev Sci Instrument* 77: 041101.
5. Wang X, Xie X, Ku G, Wang LV, Stoica G (2006) Noninvasive imaging of hemoglobin concentration and oxygenation in the rat brain using high-resolution photoacoustic tomography. *J Biomed Opt* 11: 024015.
6. ANS Institute (2014) American national standard for safe use of lasers. *Laser Institute of America*.
7. Wang L, Jacques SL, Zheng L (1995) MCML-Monte Carlo modeling of light transport in multi-layered tissues. *Comput Methods Programs Biomed* 47: 131-146.
8. Fang Q, Boas DA (2009) Monte Carlo simulation of photon migration in 3D turbid media accelerated by graphics processing units. *Opt Express* 17: 20178-20190.
9. Earl DJ, Deem MW (2008) Monte Carlo simulations. *Methods Mol Biol* 443: 25-36.
10. Wilson B, Adam G (1983) A Monte Carlo model for the absorption and flux distributions of light in tissue. *Med Phys* 10: 824-830.
11. Prahl SA, Keijzer M, Jacques SL, Welch AJ (1989) A Monte Carlo model of light propagation in tissue. *Proceedings of Dosimetry of Laser Radiation in Medicine and Biology*, Berlin Germany.
12. Blanca CM, Saloma C (1998) Monte Carlo analysis of two-photon fluorescence imaging through a scattering medium. *Appl Opt* 37: 8092-8102.
13. Turitsyn SK, Babin SA, El-Taher AE, Harper P, Churkin DV, et al. (2010) Random distributed feedback fibre laser. *Nat Photon* 4: 231.
14. Schmitt JM, Zhou GX, Walker EC, Wall RM (1990) Multilayer model of photon diffusion in skin. *J Opt Soc Am A* 7: 2141-2153.
15. Ishimaru A (1989) Diffusion of light in turbid material. *Appl Opt* 28: 2210-2215.
16. Jiang Y, Upputuri PK, Xie C, Lyu Y, Zhang L, et al. (2017) Broadband absorbing semiconducting polymer nanoparticles for photoacoustic imaging in second near-infrared window. *Nano letters* 17: 4964-4969.
17. Weissleder R. A clearer vision for in vivo imaging. *Nat Biotechnol* 19: 316-317.
18. Van Veen R, Sterenborg HJ, Pifferi A, Torricelli A, Chikoidze E, et al. (2005) Determination of visible near-IR absorption coefficients of mammalian fat using time-and spatially resolved diffuse reflectance and transmission spectroscopy. *J Biomed Opt* 10: 054004.

19. Marchesini R, Bertoni A, Andreola S, Melloni E, Sichirollo A (1989) Extinction and absorption coefficients and scattering phase functions of human tissues in vitro. *Appl Opt* 28: 2318-2324.
20. Van der Zee P (1992) Measurement and modelling of the optical properties of human tissue in the near infrared. University College London 74-07C: 318.
21. Prahl S (1999) Optical absorption of haemoglobin. Oregon Medical Laser Center.
22. Anderson RR, Parrish JA (1981) The optics of human skin. *J Invest Dermatol* 77: 13-19.
23. Bashkatov A, Genina E, Kochubey V, Tuchin V (2005) Optical properties of human skin, subcutaneous and mucous tissues in the wavelength range from 400 to 2000 nm. *J Physics D: Appl Physics* 38: 2543.
24. Treeby BE, Cox BT (2010) k-Wave: MATLAB toolbox for the simulation and reconstruction of photoacoustic wave fields. *J Biomed Opt* 15: 021314.
25. Lawandy NM, Balachandran R, Gomes A, Sauvain E (1994) Laser action in strongly scattering media. *Nature* 368: 436-438.
26. Jacques SL (1998) Light distributions from point, line and plane sources for photochemical reactions and fluorescence in turbid biological tissues. *Photochem Photobiol* 67: 23-32.